Supporting Information

Enzyme-Free Optical Detection of Uric Acid Using Corona Phase Molecular Recognition in Near-Infrared Fluorescent Single-Walled Carbon Nanotube

*Minyeong Yoon, Seyoung Shin, Seungju Lee, Soo-Yeon Cho**

School of Chemical Engineering, Sungkyunkwan University, Suwon 16419, Republic of Korea.

*Corresponding author: sooyeonc@skku.edu

Index	Sequence	Length
i	$(AAAC)_8$	32
ii	$(AAT)_{10}$	30
iii	$(ACG)_{10}$	30
iv	$(GA)_{15}$	30
v	$(GAAC)_8$	32
vi	$(GCGA)_8$	32
vii	$(GGGGT)_6$	30
viii	$(GT)_{15}$	30
ix	$(TC)_{15}$	30
x	$(TG)_{15}$	30
xi	$(AT)_{15}$	30
xii	$(ATT)_{10}$	30
xiii	A_{30}	30
xiv	T_{30}	30
xv	C_{30}	30

Table S1. List of ssDNA used in this study.

Material	Abbreviation	Molecular weight (g/mol)	Solubility (mM)
Creatine monohydrate	Cr	149.15	89.17
D-(+)-Glucose	Glu	180.16	5045.52
L-(+)-Lactic acid	LA	90.08	9547.07
L-Tyrosine	Tyr	181.19	2.48
Urea	U	60.06	highly soluble
Uric acid	UA	168.11	0.36

Table S2. List of the analytes used in this study.

Subject No.	Sex	UA concentration (μM)	pH
1	Female	5.7	6.18
2	Male	21.2	7.30
3	Male	40.2	6.00
4	Male	44.9	5.68
5	Male	67.4	6.35
6	Female	73.7	6.44

Table S3. Summary of characteristics of six human urine samples pooled for this study.

Use of enzyme	Sensing method	Material	Calibration range (μM)	LOD (nM)	Available pH	POC integration	Ref No.
Enzymatic	Colorimetry	Fe-MOF/Fe_3O_4NPs	0.2-200	180	7.4	-	1
	Electrochemistry	Nafion/UOx–ZnO NRs/Ag/glass	10-5.56×10^3	50	7	-	2
Enzyme-free	Electrochemistry	AuNPs/DNA/PSFR	0.09-12	8	5-6	-	3
	Electrochemistry	Laser-engraved graphene	6.25-200	740	4.1-5.6	Wearable sweat patch	4
	Fluorescence	Porous graphitic carbon nitride	0.05-10	8.4	7	-	5
	Fluorescence	Composite of CdTe QDs with ZIF-8	0.05-10	32	5-8	-	6
	Fluorescence	ssDNA/SWCNT	0.01-100	69	4-8	Paper strip	This work

Table S4. Comparison table of sensor performance with conventional UA detection sensors.

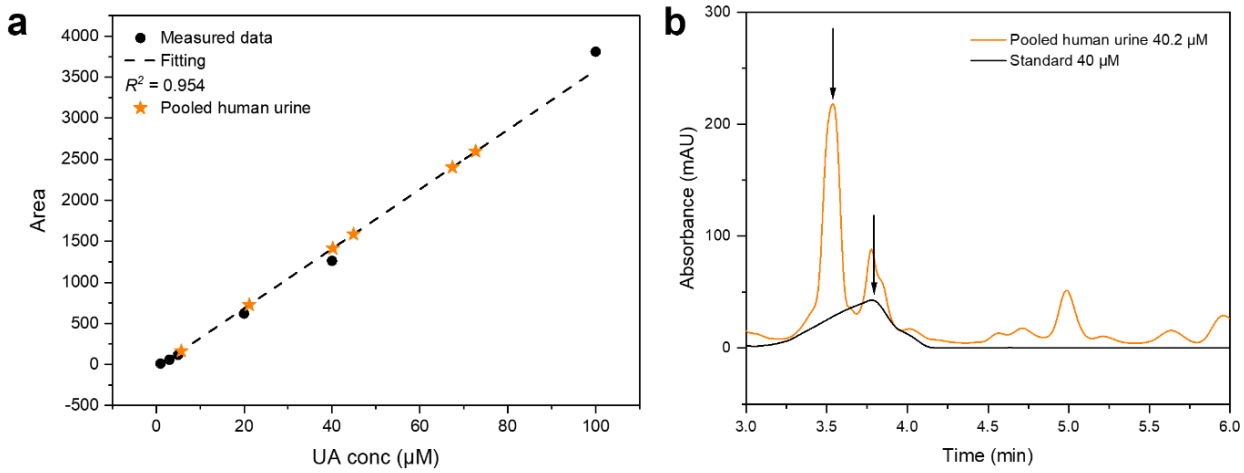

Figure S1. HPLC data for determining UA concentration of pooled human urine. (a) Calibration curve generated using standard UA solutions at 1, 3, 5, 20, 40, and 100 μM. (b) Absorbance spectrum at 290 nm for human urine containing 40.2 μM of UA and a standard 40 μM UA solution. [7] The spiked peaks, indicated by the black arrows, represent the strongest signals within the significant retention time range from standard UA solutions and were used to determine UA concentrations of the human urine samples before using for study. The variation might be due to the matrix differences in urine samples (orange line) and the standard solution based on DI:methanol = 9:1 (black line).

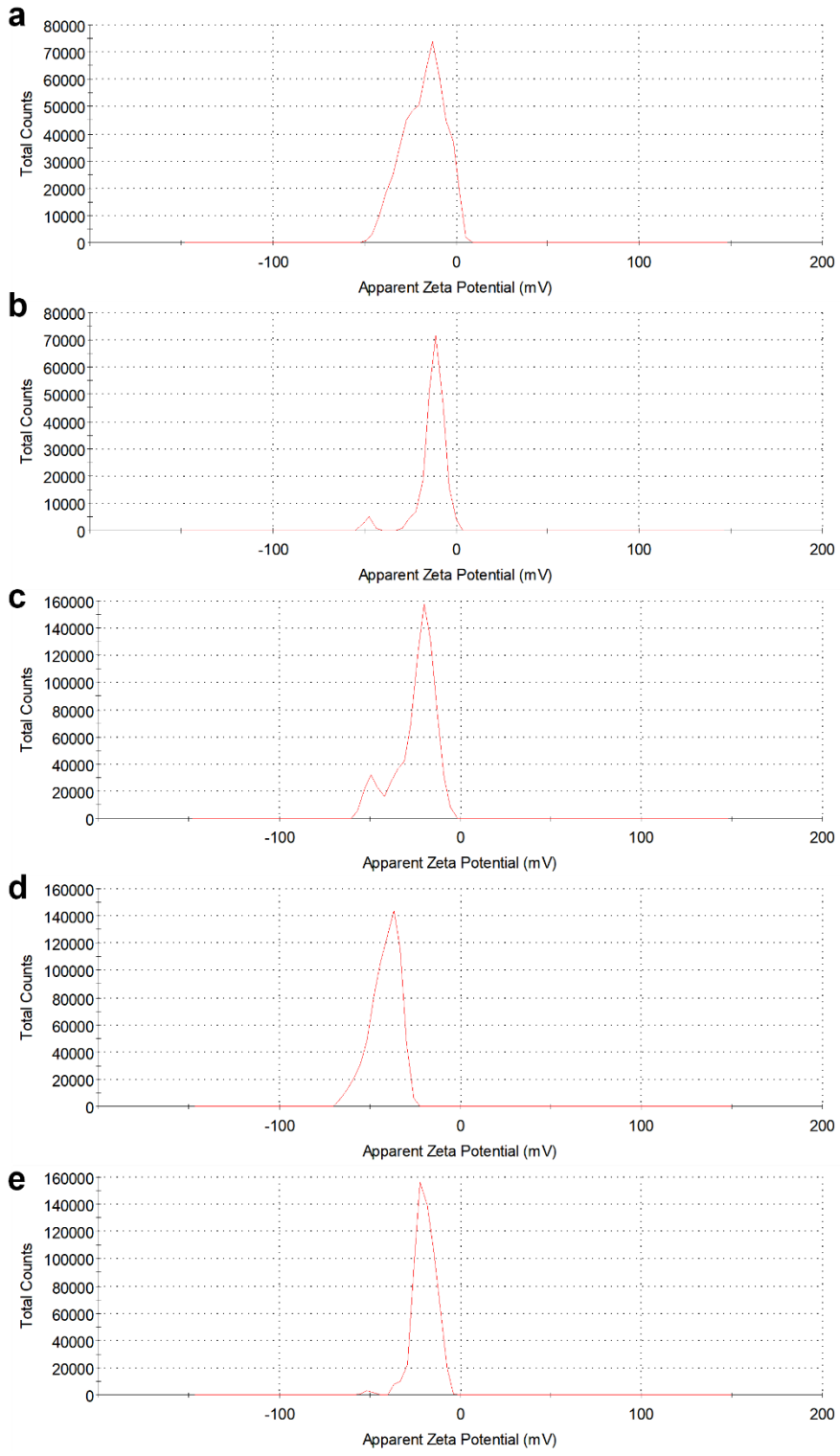

Figure S2. Zeta potential distribution of unbuffered $(AAT)_{10}$/SWCNT nanosensor with addition of pH buffers as a sensor-to-buffer ratio of 9:1. (a) pH 4. (b) pH 5. (c) pH 6. (d) pH 7. (e) pH 8.

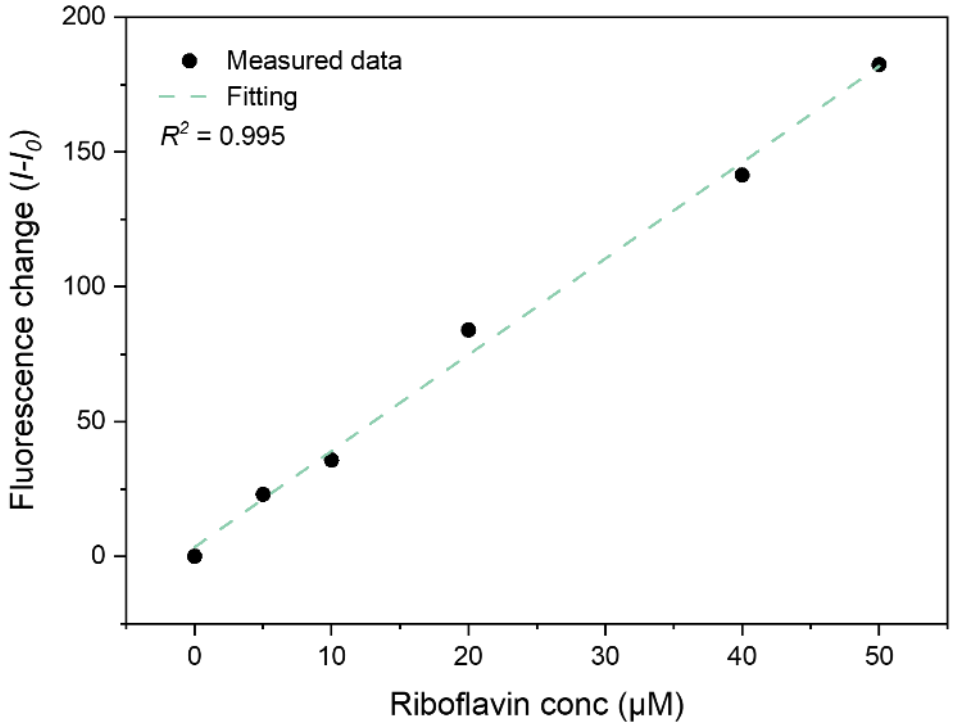

Figure S3. Fluorescence intensity of riboflavin measured at its maximum spectral peak across various concentrations.

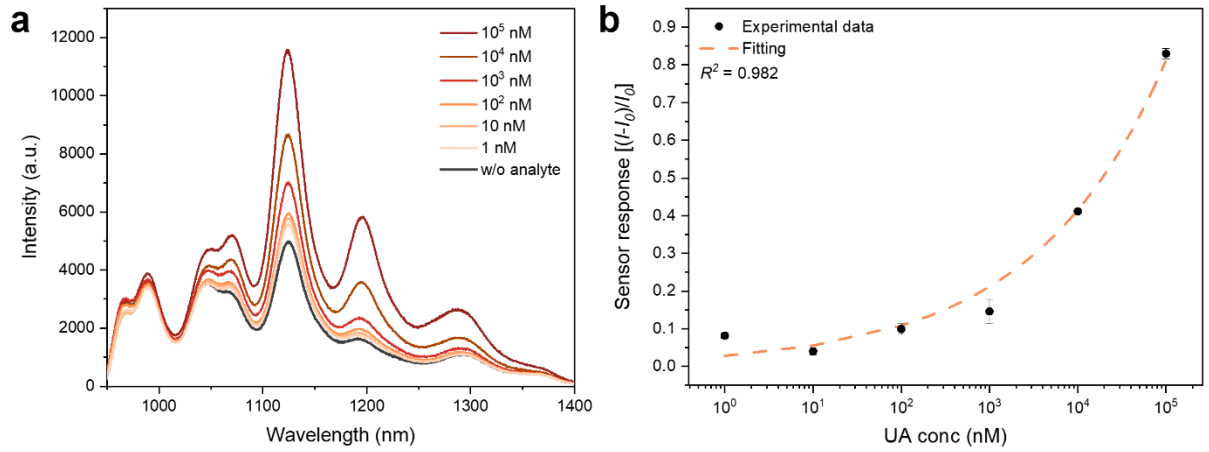

Figure S4. Preserved buffered $(AAT)_{10}$/SWCNT nanosensor performance with analytes in pH 4 buffers. (a) Fluorescence spectra of the corona nanosensor diluted in PBS in response to 1 – 10^5 nM UA in pH 4 buffers. (b) Calibration curve of the corona nanosensor diluted in PBS with 1 – 10^5 nM UA in pH 4 buffers (n = 3).

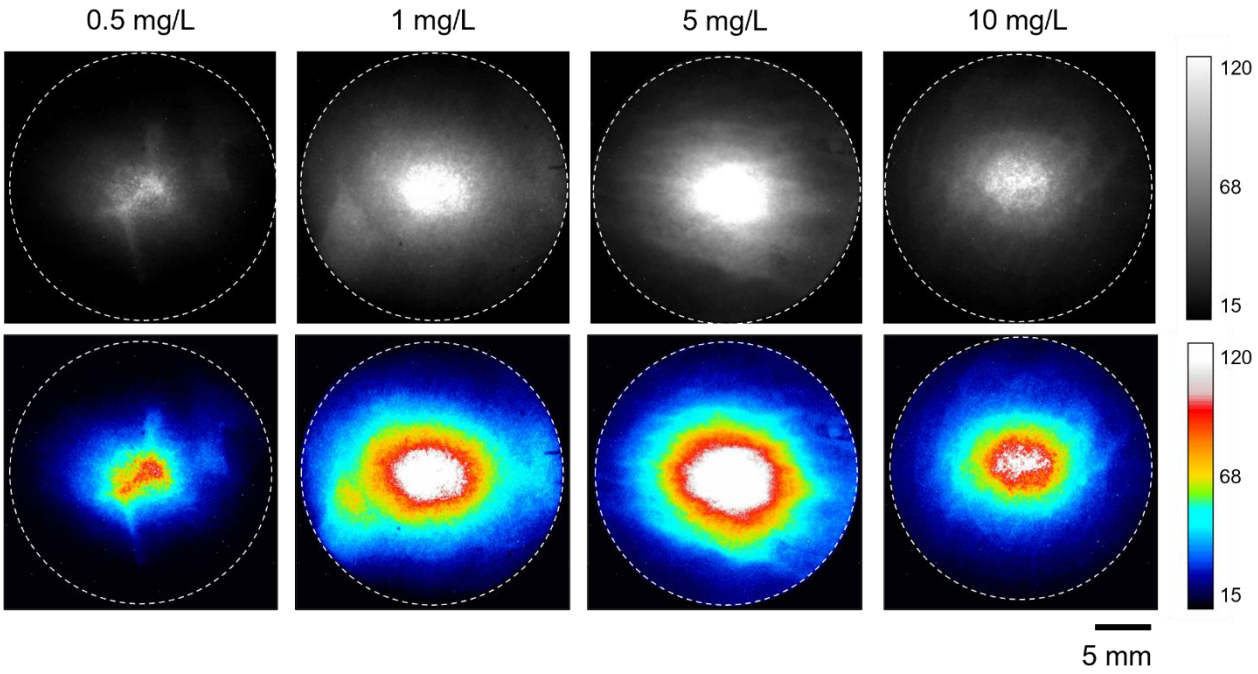

Figure S5. nIR images of PES substrates coated with the $(AAT)_{10}$/SWCNT nanosensor solutions at concentrations of 0.5, 1, 5, and 10 mg/L (from left to right).

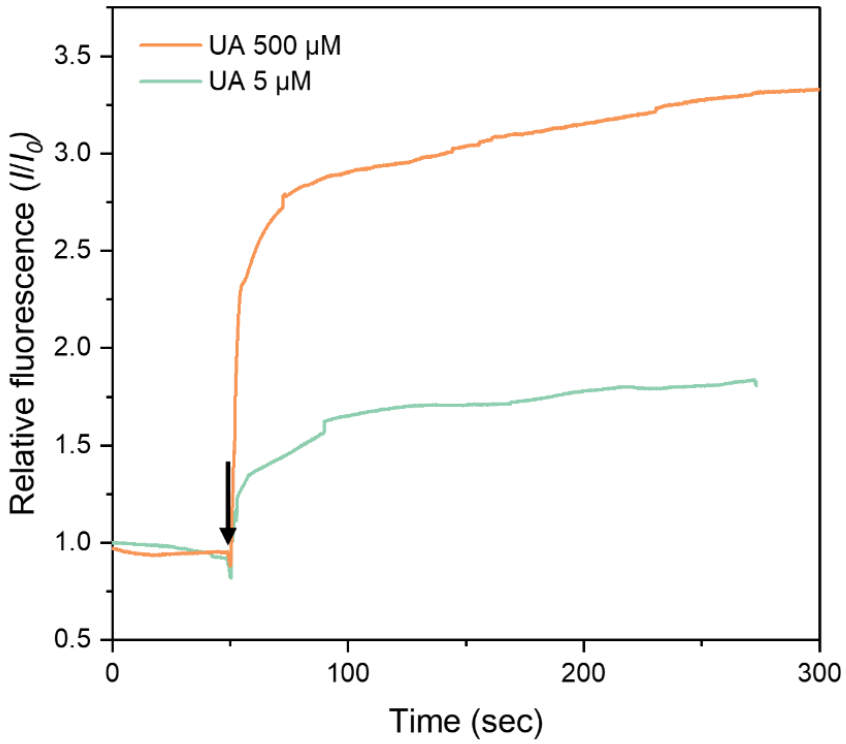

Figure S6. Fluorescence changes of the optical test strip after the addition of pooled human urine containing UA at 5.7 and 500 μM, with input introduced at 50 sec.

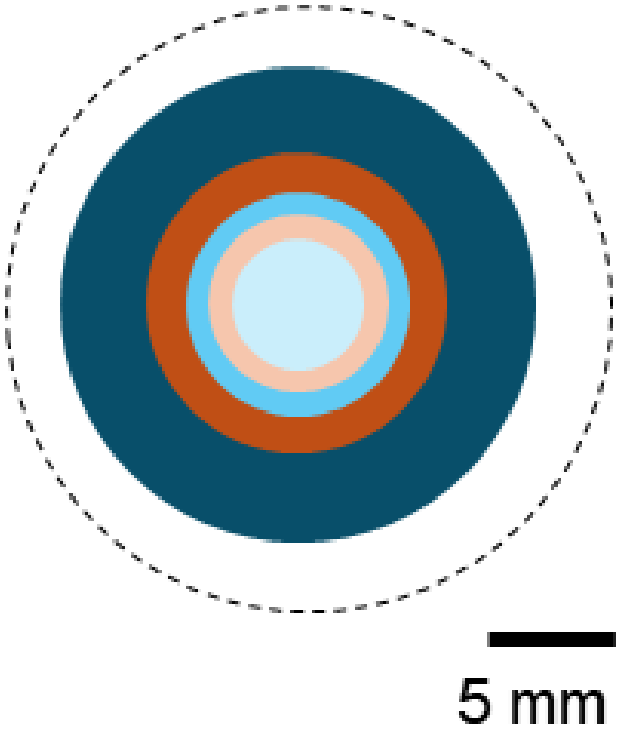

Figure S7. Valid reaction area distribution induced by solution spreading on the sample shown in **Fig. 4d** with time at 0, 1, 2, 5, 30 sec.

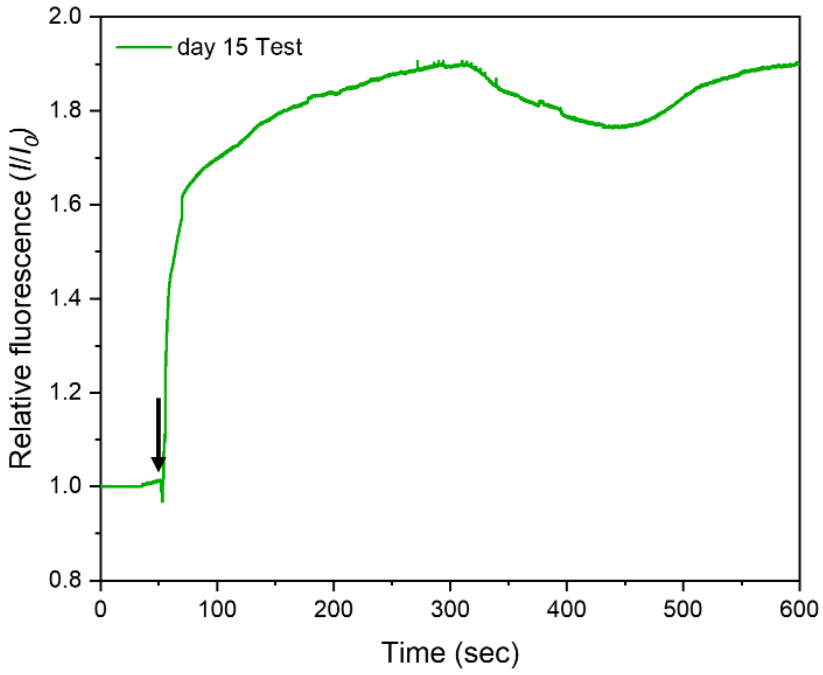

Figure S8. Fluorescence changes of the optical test strip after 15 days of storage, following the input of UA 100 μM in DI water at 50 sec.

References

1. T. Lian, J. Chen, X. Tang, P. Qiu and Y. Hu, *Microchemical Journal*, 2024, **196**, 109538.
2. R. Ahmad, N. Tripathy, M.-S. Ahn and Y.-B. Hahn, *Scientific Reports*, 2017, **7**, 46475.
3. L. M. Niu, K. Q. Lian, H. M. Shi, Y. B. Wu, W. J. Kang and S. Y. Bi, *Sensors and Actuators B: Chemical*, 2013, **178**, 10-18.
4. Y. Yang, Y. Song, X. Bo, J. Min, O. S. Pak, L. Zhu, M. Wang, J. Tu, A. Kogan, H. Zhang, T. K. Hsiai, Z. Li and W. Gao, *Nature Biotechnology*, 2020, **38**, 217-224.
5. Y. Yang, W. Lei, Y. Xu, T. Zhou, M. Xia and Q. Hao, *Microchimica Acta*, 2018, **185**, 1-9.
6. X. Zheng, Y. Yang, F. Gao, H. Li, W. Yang, D.-Y. Guo, S. Chen and Q. Pan, *Microchimica Acta*, 2022, **189**, 435.
7. N. Norazmi, Z. A. Rasad, M. Mohamad and H. Manap, *IOP Conference Series: Materials Science and Engineering*, 2017.